Fluid Dynamics &
Materials Processing

Tech Science Press

http://doi.org/10.32604/fdmp.2026.079864

ARTICLE

Effective Pore-Throat Sweep Limits and Microscopic Oil Mobilization during CO_2-WAG Flooding in Low-Permeability Conglomerate Reservoirs

Xiaoguang Wang[1,2], Dehua Liu[1,2,*], Zhenping Liu[3], Zhen Luo[3], Guihua Yang[1,2], Zongfa Li[1,2] and Lijuan Huang[1,2,*]

[1]State Key Laboratory of Low Carbon Catalysis and Carbon Dioxide Utilization (Yangtze University), Wuhan, China
[2]School of Petroleum Engineering, Yangtze University, Wuhan, China
[3]Research Institute of Exploration and Development, Xinjiang Oilfield Company, PetroChina, Karamay, China
*Corresponding Authors: Dehua Liu. Email: dh.liu@tom.com; Lijuan Huang. Email: huanglijuan@yangtzeu.edu.cn

Received: 29 January 2026; Accepted: 11 June 2026; Published: 31 July 2026

ABSTRACT: Low-permeability conglomerate reservoirs are characterized by complex pore structures and poor sweep efficiency, making the optimization of carbon dioxide-water alternating gas (CO_2-WAG) injection critical for enhanced oil recovery. To evaluate the displacement performance of CO_2-WAG and determine the lower limit of effectively swept pore throats, this study presents long-core flooding experiments conducted on cores from the KS Formation of the B Oilfield in the Junggar Basin under reservoir conditions (20.1 MPa and 58°C). Continuous CO_2 flooding and CO_2-WAG schemes with varying cycle numbers and gas-water ratios (GWRs) were systematically compared. *In situ* online nuclear magnetic resonance (NMR) monitoring was employed to quantitatively characterize the mobilization of microscopic remaining oil during flooding. The results demonstrate that CO_2-WAG significantly outperforms continuous CO_2 flooding. Among the tested scenarios, three alternating cycles and a GWR of 1:1 yielded the highest oil displacement efficiencies of 64.8% and 66.13%, respectively, representing improvements of 23.6% and 24.53% over water flooding and 4.75% and 6.08% over continuous CO_2 flooding. NMR analysis revealed that water flooding primarily mobilizes crude oil in larger pore throats, with an effective sweep limit of approximately 18.2 nm. In contrast, CO_2-WAG extends the lower limit of effectively swept pore throats to 9.52 nm, enabling the recovery of oil trapped within mesopores and micro/nano-scale pore systems. Mechanistically, the injected water slugs improve sweep efficiency and suppress gas channeling, while the CO_2 slugs reduce crude oil viscosity and enhance displacement within smaller pores. This synergistic combination of macroscopic sweep improvement and microscopic displacement enhancement substantially increases oil recovery.

KEYWORDS: CO_2-WAG; conglomerate reservoirs; oil displacement efficiency; nuclear magnetic resonance; producing limit

1 Introduction

The tight structure, pronounced heterogeneity, low porosity, and low permeability of conglomerate reservoirs render conventional water flooding and gas flooding methods inefficient and difficult to implement effectively. Reservoir B, a representative conglomerate reservoir in the Junggar Basin, is characterized by poor petrophysical properties, strong heterogeneity, and high sensitivity. Its development performance has declined progressively in recent years, while the issue of ineffective water injection circulation has become increasingly prominent. The reservoir has entered a "double-high" development stage and urgently requires a transformation of the development strategy to further enhance the recovery factor.

CO_2 injection is an effective approach for recovering substantial amounts of oil from low-permeability or tight reservoirs [1,2]. However, the sweep volume achieved during CO_2 flooding has consistently remained a critical challenge. The unfavorable mobility ratio between CO_2 and crude oil, mainly caused by the large viscosity contrast between the two phases, generally results in reduced sweep efficiency within the reservoir. In the absence of effective profile control, viscous fingering, channeling, premature CO_2 breakthrough, and crude oil bypassing can further impair the macroscopic sweep efficiency of CO_2 flooding, thereby significantly reducing both CO_2 utilization and storage efficiency [3].

Controlling the unfavorable mobility ratio during gas injection to improve macroscopic sweep efficiency has long been a major research focus. CO_2-WAG has been applied in heterogeneous reservoirs as an important zero-carbon or even carbon-negative technology for mitigating gas channeling and viscous fingering during CO_2-enhanced oil recovery. For heterogeneous low-permeability reservoirs with complex seepage mechanisms, alternating CO_2 and water injection (WAG) can regulate fluid flow at the displacement front to some extent and suppress gas viscous fingering, thereby improving CO_2 sweep efficiency and enhancing flooding performance [4]. This technique combines the expanded sweep volume associated with water flooding and the high displacement efficiency of CO_2 injection. In addition, WAG injection may promote bubble formation within the reservoir, creating high flow resistance in swept zones through the Jamin effect and diverting more displacing fluid into unswept regions, thereby further improving macroscopic sweep efficiency.

The water-alternating-gas (WAG) technique has progressively matured through laboratory physical simulation studies and field applications, and it is now recognized as one of the most effective enhanced oil recovery (EOR) methods for low-permeability reservoirs. Extensive research has been conducted on its principal design parameters and influencing factors, including gas–water ratio, number of WAG cycles, slug size, injection rate, oil–gas phase behavior, and gas type [5–8]. Fang et al. [9] reviewed recent advances in CO_2-water-alternating-gas (CO_2-WAG) technology for enhanced oil recovery, covering its theoretical basis, field applications, fluid displacement mechanisms, and control strategies. Abdurrahman et al. [10], focusing on the Sumatera Light Oilfield, performed numerical simulations of immiscible alternating CO_2 and water injection and reported that a gas–water ratio of 1:2 was optimal, yielding an incremental recovery factor of 35.24%. When the gas–water ratios were 2:1 and 1:1, the additional recovery factors were 1.49% and 19.52%, respectively. Khather et al. [11] established residual oil saturation after water flooding under reservoir conditions and subsequently injected CO_2 and reconstituted formation water alternately (0.5 pore volume CO_2 and 0.5 pore volume water). Porosity, permeability, NMR T_2 measurements, and X-ray CT scans were conducted before and after the experiment. The results showed that CO_2-WAG significantly increased oil recovery by approximately 30% under the tested conditions. Zhang et al. [12] investigated the enhanced recovery mechanism of CO_2-WAG through displacement experiments using cores with different permeability levels to simulate heterogeneous reservoirs. Nuclear magnetic resonance (NMR) technology was used to monitor the dynamic distribution of residual oil during displacement at multiple scales, including reservoir, layer, and pore scales. The effects of gas–water ratio and injection rate on multiscale recovery were also evaluated. CO_2-WAG effectively suppressed early breakthrough in high-permeability layers, improved displacement efficiency in medium- and low-permeability layers, and enhanced microscopic displacement efficiency in medium and small pores. Al-Bayati et al. [13] evaluated the possible evolution of petrophysical properties in layered sandstone core samples during miscible CO_2-WAG injection. Porosity and pore-size distribution were measured using NMR before and after water injection. Li et al. [14] found experimentally that CO_2-WAG significantly altered the distribution of residual oil, and increasing the number of WAG cycles could further improve oil production. After water flooding,

CO_2 preferentially entered highly water-saturated pore throats and formed trapped gas, thereby reducing water production while increasing crude oil recovery. In that study, microfluidic visualization experiments were used to observe fluid flow behavior and residual oil mobilization in low-permeability reservoirs during alternating injection of CO_2, water, and gas after water flooding. Sang et al. [15] proposed that CO_2 injection reduced crude oil adhesion and interfacial tension, disrupted the oil–water equilibrium, and increased local displacement pressure, thereby improving the utilization of residual oil. With increasing WAG cycles, the productive pore-throat range remained within 8–30 μm, and residual oil displacement efficiency continued to improve, revealing the recovery mechanism of alternating CO_2 and water flooding in low-permeability reservoirs. Liu et al. [16] combined core flooding experiments with NMR analysis to investigate the enhanced recovery mechanism of CO_2-WAG at multiple scales, including reservoir, layer, and pore scales. The study compared sandstone and conglomerate reservoirs under miscible and immiscible conditions and analyzed the effects of gas–water ratio and injection rate. Under immiscible conditions, CO_2-WAG achieved an oil recovery factor of approximately 22.95%, which was 7.82% higher than that of continuous CO_2 flooding. This method effectively suppressed CO_2 breakthrough in high-permeability layers while increasing recovery in medium- and low-permeability zones. As the gas–water ratio increased, total oil recovery also increased, together with improved recovery in low-permeability layers and micropores.

Xu et al. [17] combined NMR and CT techniques to study the microscopic distribution and displacement mechanism of residual oil during alternating CO_2 and water injection in water-sensitive tight reservoirs. CO_2 dispersed oil droplets, most of which were displaced from the pores, whereas water served as a mobility-control phase by blocking larger pores. However, due to water sensitivity, mesopores and micropores were also impaired, resulting in only marginal improvement from WAG following the initial CO_2 flooding. Lang et al. [18] investigated factors influencing CO_2 flooding in shale reservoirs through NMR experiments and analyzed the effects of soaking time, pressure, and temperature on CO_2 flooding recovery based on NMR T_2 spectra. Li et al. [19] conducted pore-scale simulations of WAG injection in water-wet porous media. The results showed that alternately injected water and gas preferentially swept the lower and upper regions of the porous medium, respectively, thereby increasing oil recovery compared with standalone water flooding or gas flooding. In particular, WAG processes ending with gas flooding showed considerable potential for both EOR and CO_2 sequestration. For fixed injection cycles, increasing the volume of individual slugs further enhanced oil recovery. Using natural dense core samples from the Ordos Basin and high-precision NMR monitoring techniques, Zheng et al. [20] found that CO_2-WAG increased flow resistance by 3 to 8 times compared with continuous displacement. Meanwhile, oil recovery increased by 5.1% to 9.0%, and sequestration efficiency improved by 4.3% to 5.6%. The combined CO_2 utilization and storage coefficient reached its highest value, and the optimal segmented sequestration ratio was determined to be 1:1. Further analysis combined with MRI results indicated that during alternating CO_2 and water injection, the injected water preferentially occupied dominant flow channels or fractures, thereby delaying gas breakthrough through the Jamin effect. Wang et al. [21] selected three representative conglomerate cores from different layers and conducted CO_2 flooding and CO_2-WAG flooding experiments using NMR technology. The results showed that immiscible CO_2 flooding mainly displaced crude oil in large pores, whereas crude oil in micropores and mesopores was difficult to mobilize. After gas channeling occurred, extensive clusters of residual oil still remained in the cores, resulting in low recovery factors. He et al. [22] conducted long-core displacement experiments on CO_2-WAG by adjusting alternating cycle size. NMR techniques were used to quantitatively characterize oil displacement performance under different microscopic pore structures. The results showed that during CO_2-WAG flooding, cores with medium to high permeability exhibited higher recovery factors than those with medium to low permeability. CO_2-WAG effectively mitigated gas channeling in medium- to high-permeability heterogeneous reservoirs. Wang et al. [23] conducted comparative experiments on CO_2 flooding and alternating CO_2-water flooding in the same multilayer system under miscible conditions (70°C, 18 MPa). After continuous CO_2 flooding, the overall crude oil recovery factor was only 27.6%, with production mainly originating from the high-permeability layer, while the remaining oil was largely retained in medium- and low-permeability layers. In contrast, CO_2-WAG required higher injection pressure but delayed CO_2 breakthrough, and the total recovery factor increased to 44.5%. The contribution rates of the medium- and low-permeability layers to oil production increased to 3.8% and 17.1%, respectively. Through microscopic experiments, Qin et al. [4] found that the presence of gas in large pores altered the flow path of water during the second water-flooding cycle. Consequently, the enlarged sweep volume combined with favorable microscopic displacement efficiency demonstrated the high effectiveness of CO_2-WAG injection.

The results of relevant studies on oil displacement efficiency and lower limit of effectively swept pore throats in low-permeability reservoirs seem insufficient. Studies generally suggest that alternating cycles and gas-water ratio are key parameters for optimizing the WAG effect. Therefore, in view of the high water cut, low permeability and strong heterogeneity of the ultra-low permeability of the conglomerate reservoir in oilfield B, this paper used an indoor long core experimental setup and on-site retrieved actual core splicing to simulate multiple sets of comparative experiments of continuous gas flooding and different alternating cycles and different gas-water ratio of CO_2-WAG under formation temperature of 58°C and formation pressure of 20.1 MPa in B reservoir, The oil displacement effect and mechanism of CO_2-WAG were studied, and the injection parameters for CO_2-WAG flooding were optimized to provide a technical basis for its field application in the target reservoir. In addition, there is a lack of *in-situ* and quantitative understanding of how CO_2-WAG utilizes crude oil from the denser micropores (especially nanoscale pores) in low-permeability reservoirs. For the KS group core, the lower limit of effectively swept pore throats was calibrated through online nuclear magnetic resonance experiments, and the synergistic mechanism of WAG was revealed.

2 Experimental Equipment, Materials and Methods

2.1 Core Displacement Experiments

2.1.1 Experimental Equipment

As shown in Fig. 1, the CO_2-water alternating displacement system comprises an injection pump, a back-pressure regulator (BPR), three intermediate containers (for oil, gas and water, respectively), a core holder, a back pressure regulator, an oil-gas water separator and a metering device. The upper limit of working pressure for the displacement system is 70 MPa. The core holder and three intermediate containers are located in the oven. High-pressure stainless steel core holders are used to hold the core samples, which are mounted in the center of the core holder via rubber sleeves. Use three piston cylinders to store the experimental fluids (oil, water, and CO_2). During the experiment, the fluid was injected into the core through a steel pipeline by a dual-plunger pump, and the injection pressure was measured by a pressure gauge installed at the inlet of the core holder. Set the confining pressure to prevent the experimental fluid from flowing around the core. Confining pressure was applied to prevent fluid bypassing the core sample. Additionally, a back pressure regulator (BPR) was installed at the outlet of the core holder to maintain the preset experimental pressure. The produced oil and water are collected in an oil-water separator.

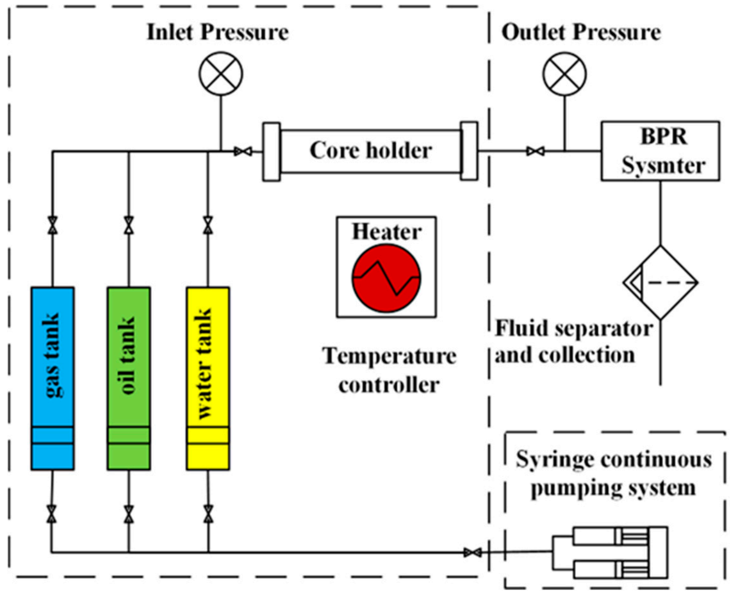

Figure 1: The sketch of CO_2-WAG flooding system.

2.1.2 Experimental Materials

(1) Reservoir fluids

The crude oil was obtained from the KS formation oil reservoir of B Oilfield in the Ordos Basin. The MMP for the reservoir fluid and CO_2 was determined to be 18.5 MPa via slim tube experiments. The original formation pressure of the oil reservoir was 20.1 MPa, the pressure coefficient was 1.06, the temperature in the middle of the oil layer was 58°C, and the saturation pressure was 15.4 MPa. The original dissolved gas-oil ratio is 87 m^3/m^3 and the volume coefficient is 1.211. Formation crude oil viscosity 1.86 mPa·s density 0.768 g/cm^3. Surface crude oil has a density of 0.8379 g/cm^3, a pour point of 10.9°C, and a wax content of 7.6 percent. Specific gravity of associated natural gas 0.7893. Formation water type $NaHCO_3$, total dissolved solids: 3574–6810 mg/L. The purity of the CO_2 used in the experiment was 99.99%.

(2) Core samples

Three cores with a diameter of 3.8 cm from the KS reservoir were selected and connected in series, with a length of 19.237 cm after splicing (Fig. 2). Filter paper was used to connect the end faces of the shorter cores. The average permeability of the core was 4.22 mD. The cores with the permeability closest to the average were placed in sequence near the outlet end, and the core parameters are shown in Table 1.

Figure 2: Core of the KS formation in the conglomerate reservoir.

Table 1: Core parameters.

Core Number	Depth	Diameter/mm	Length/mm	Permeability/mD	Porosity/%
8	1935.60	38.42	76.17	4.56	8.97
6	1931.77	38.43	54.73	6.32	13.55
1	1938.40	38.42	61.47	1.78	8.67

2.1.3 Experimental Methods

The experimental steps for continuous CO_2 displacement and gas-water alternating displacement are as follows:

(1) Preparation of the experimental fluid:

After sampling the oil and gas samples from the surface separator in oilfield B, they were miscible and thoroughly stirred and balanced (~4 h) under formation temperature and pressure to make the fluid mixture a single-phase fluid.

(2) Core preparation:

Prepare the long core holder, load the cores into the long core holder in the required sequence, calibrate, clean and dry the instrument, test the temperature and pressure, then evacuate and bring it to 58°C.

(3) Saturated formation water:

Control the inlet pump to inject the reconstituted formation water into the long core, establish the system pressure of the long core to the formation pressure of 20.1 MPa, record the pump value, and calculate the saturated water volume of each long core.

(4) Establish the irreducible water saturation and the original formation conditions:

Use live oil to replace the formation water to establish the irreducible water saturation of the long core. When the gas-oil ratio at the outlet end is consistent with the sample preparation, the original formation conditions are established, and then aging is carried out.

(5) Water flooding:

Inject formation water at 0.1 mL/min at the inlet end and record the oil and water production at the outlet end.

(6) (6.1) Pure CO_2 flooding:

After water flooding to a Water cut >95%, inject CO_2 at 0.1 mL/min until no oil is produced or only gas is produced. Record the oil production, water production and gas production, and calculate the flooding efficiency.

(6.2) CO_2-water alternate flooding:

Carry out CO_2-water alternate flooding after water flooding to a Water cut >95%. When exploring the influence of cycle, the total injection volume for each alternate round is designed to remain constant at 2 PV, and 1 to 5 cycles of displacement experiments are carried out at a gas-water ratio of 1:1. When exploring the influence of gas-water ratio, the total injection volume of CO_2 was maintained at 1 PV, and the gas-water ratio range was designed to be 2:1 to 1:2. CO_2 and water slugs were injected alternately at 0.1 mL/min until no oil was produced/only gas was produced. Record the production of oil and water, and calculate the oil displacement efficiency. Experimental protocols are shown in Tables 2 and 3.

(7) Cleaning the core:

After the experiment, the core was cleaned with petroleum ether and anhydrous alcohol. The petroleum ether was mainly used to clean the oil in the core, and the anhydrous alcohol was used to clean the water in the core. After cleaning, repeat steps (1)–(5) to form the original state for the next set of experiments.

Table 2: Water and gas alternate displacement experiment schemes for different alternating cycles.

Experiment Number	Experiment Type	Cycles of Experiments	Experimental Protocol
1	Water drive	/	1 PV
2	CO_2-WAG	1 cycle	1 PV CO_2 + 1 PV water
3	CO_2-WAG	2 cycles	0.5 PV CO_2 + 0.5 PV water
4	CO_2-WAG	3 cycles	0.33 PV CO_2 + 0.33 PV water
5	CO_2-WAG	4 cycles	0.25 PV CO_2 + 0.25 PV water
6	CO_2-WAG	5 cycles	0.2 PV CO_2 + 0.2 PV water

Table 3: Experimental schemes for alternating water and gas displacement with different gas-water ratio.

Experiment Number	Experiment Type	Gas-Water Ratio	Experimental Protocol
1	Water drive	/	1 PV
2	CO_2-WAG	2:1	0.25 PV CO_2 + 0.13 PV water
3	CO_2-WAG	1.5:1	0.25 V CO_2 + 0.17 PV water
4	CO_2-WAG	1:1	0.25 PV CO_2 + 0.25 PV water
5	CO_2-WAG	1:1.5	0.25 PV CO_2 + 0.38 PV water
6	CO_2-WAG	1:2	0.25 PV CO_2 + 0.5 PV water

2.2 Online Nuclear Magnetic Resonance Experiments

2.2.1 Laboratory Equipment

Through nuclear magnetic resonance relaxation analysis, the variation patterns of reservoir seepage characteristics under formation temperature and pressure conditions can be studied. As show in Fig. 3, the specification of the equipment is Niumag MacroMR12-150H-I. Magnetic field intensity 0.3 T, pulse frequency 1 to 30 MHz, frequency control accuracy up to 0.1 Hz, pulse accuracy 100 ns. The radio frequency has a maximum sampling bandwidth of 2000 KHz. The minimum echo time for a 1.5-inch core is 200 μs.

Figure 3: Online nuclear magnetic resonance displacement experimental apparatus.

2.2.2 Experimental Materials

The nuclear magnetic displacement experiment used the 9# core of the KS formation (Fig. 4), with a formation depth of 1931.97 m, a length of 72.12 mm, a diameter of 38.42 mm, a porosity of 10.43%, and a permeability of 3.10 mD. The injected water was a 6% mass fraction of manganese chloride solution. This causes the water signal to be shielded during the MRI scan, allowing only the detecting only the residual oil signal, thus making the results more accurate.

Figure 4: Conglomerate core from the online NMR experiment.

2.2.3 Experimental Methods

(1) Core pretreatment:

Oil washing and drying of tight reservoir cores sampled on-site;

(2) Saturated compound oil:

Place the core in an intermediate container, then vacuum for 48 h, and saturate the compound oil in the intermediate container for 48 h to saturate the crude oil into the throat of the tight reservoir core;

(3) T_2 spectrum of saturated oil state core:

Remove the core from the intermediate container and test the NMR T_2 spectrum in the saturated oil state;

(4) Water displacement T_2:

Place the conglomerate core in the core holder of the set displacement system at a temperature of 58°C, and apply back pressure to the end of the core holder to a formation pressure of 20.1 MPa. Water is injected into the core holder at a constant rate of 0.1 mL/min. The confining pressure of the core holder is always 2.0 MPa higher than the pressure at the injection end. Water is injected for displacement until no oil is produced.

(5) CO_2 continuous displacement T_2 spectra:

Insert the conglomerate core into the core holder in the established displacement system, set the temperature at 58°C, and apply back pressure to the end of the core holder to the formation pressure of 20.1 MPa. CO_2 gas was injected into the core holder at a constant rate of 0.1 mL/min. The confining pressure of the core holder was always 2.0 MPa higher than the pressure at the injection end until the oil volume recorded in the graduated cylinder at the end of the core no longer increased, and the displacement experiment was concluded. Test the nuclear magnetic resonance T_2 spectra under different continuous CO_2 displacement states;

(6) Replace the displacement medium:

Use a constant injection rate of 0.1 mL/min to alternately inject CO_2 and water slugs of a 1:1 gas-water ratio into the core holder to replace crude oil in the core of the gravel reservoir, and repeat steps (2) to (5);

(7) Data processing:

Convert the NMR T_2 spectrum into the pore throat distribution to characterize the crude oil usage in pore throats of different sizes. The relationship between the T_2 value of the fluid in the rock pores and the pore diameter can be expressed as:

$$T_2 = Cr \tag{1}$$

$$C = 1/\rho F \tag{2}$$

here, ρ represents the surface relaxation rate of the rock core, and F is the pore shape factor. The surface relaxation rate is obtained from the data of high-pressure mercury porosimetry.

3 Core Displacement Experiments with Different CO_2 Injection Methods under Formation Conditions

(1) Continuous CO_2 displacement and CO_2-WAG displacement in different cycles

To see how the number of alternating cycles affects the CO_2-WAG performance, displacement experiments were run on the KS group core with 1 to 5 cycles. Figs. 5–10 show the results of experiments using cores from the KS group. The injection rate was kept constant at 0.1 mL/min. A gas-water ratio of 1:1 was used. The changes in oil displacement efficiency, water cut, and gas-oil ratio over time were recorded. The changes in oil production, water production, and gas production with injected pore volume were also measured. These experiments simulated reservoir formation conditions at 20.1 MPa and 58°C. Waterflooding was performed until the water cut went above 95%. After that, CO_2 was injected. This step clearly raised the oil displacement efficiency. The error bars in the figures show a data error of 3%. The irreducible water saturation was 36.3%. The water cut reached 95% at 1 PV. At that point, the oil displacement efficiency was 41.30%. Then continuous CO_2 displacement was carried out. Gas broke through at 1.27 PV. The cumulative oil displacement efficiency at breakthrough was 43.78%. Gas injection was continued to 2.03 PV. Then the oil recovery efficiency became stable. The final oil displacement efficiency after gas flooding reached 60.05%. This value was 18.75% higher than the value after water flooding. The gas-oil ratio at the end was 6454 m^3/m^3. The experimental results confirmed that CO_2 flooding has a clear potential for enhanced oil recovery. However, the high gas-oil ratio also pointed to a tendency for gas channeling. The injection strategy needs more work to improve sweep efficiency. To assess the potential formation damage caused by CO_2-WAG injection, the permeability of the long cores was remeasured after the experiments. Results indicated no significant formation damage; instead, the average permeability slightly increased by approximately 5%. This phenomenon is likely attributed to the dissolution of carbonate cementing materials by carbonic acid generated during the CO_2 flooding process.

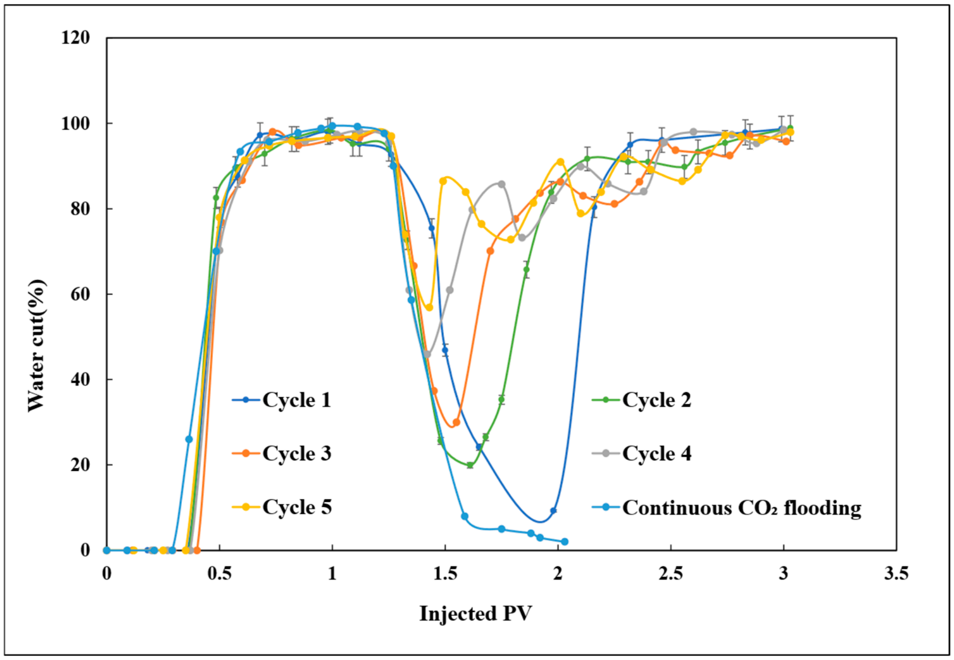

Figure 5: Water cut of KS core under continuous CO_2 flooding and different WAG cycles.

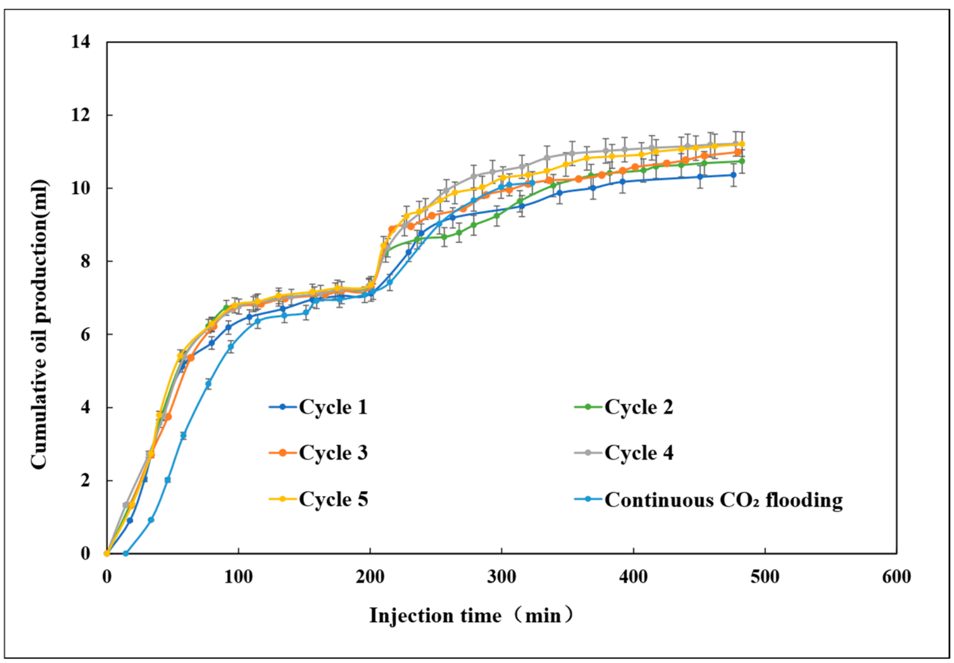

Figure 6: Cumulative oil production of KS core under continuous CO_2 flooding and different WAG cycles.

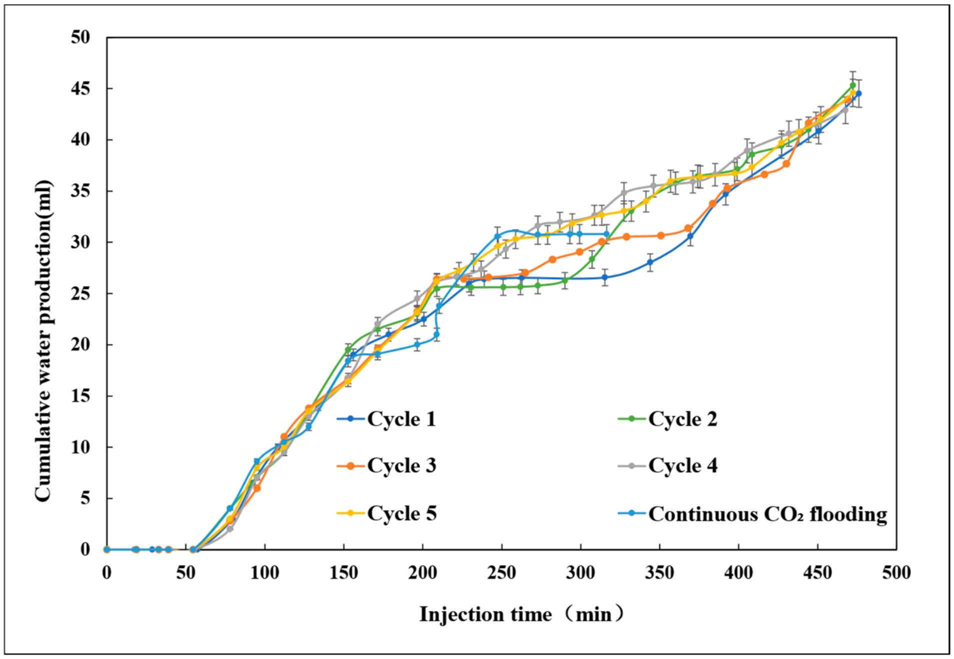

Figure 7: Cumulative water production of KS core under continuous CO_2 flooding and different WAG cycles.

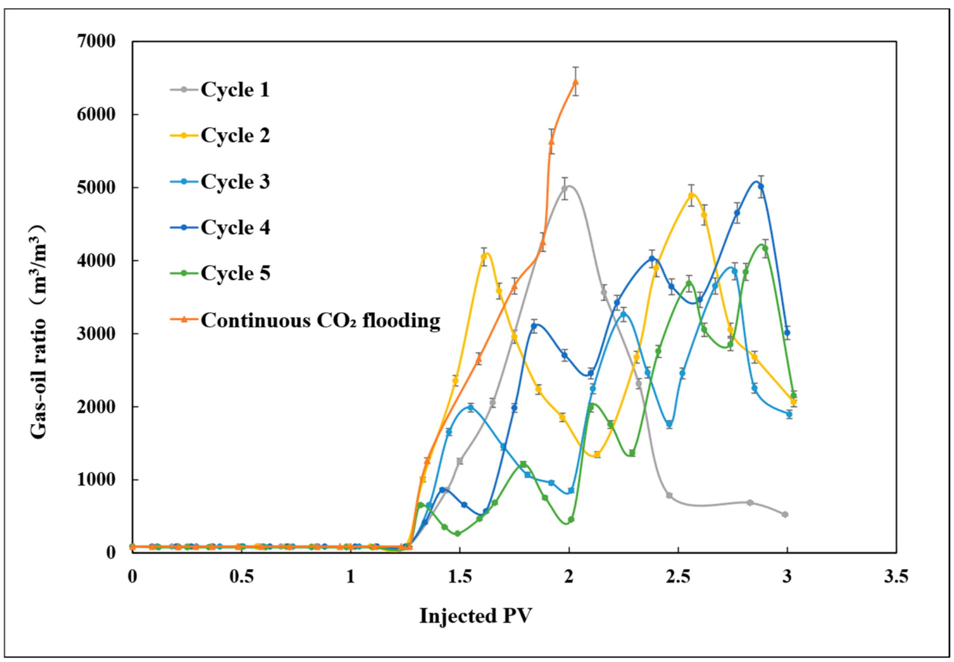

Figure 8: Gas-oil ratio of KS core under continuous CO_2 flooding and different WAG cycles.

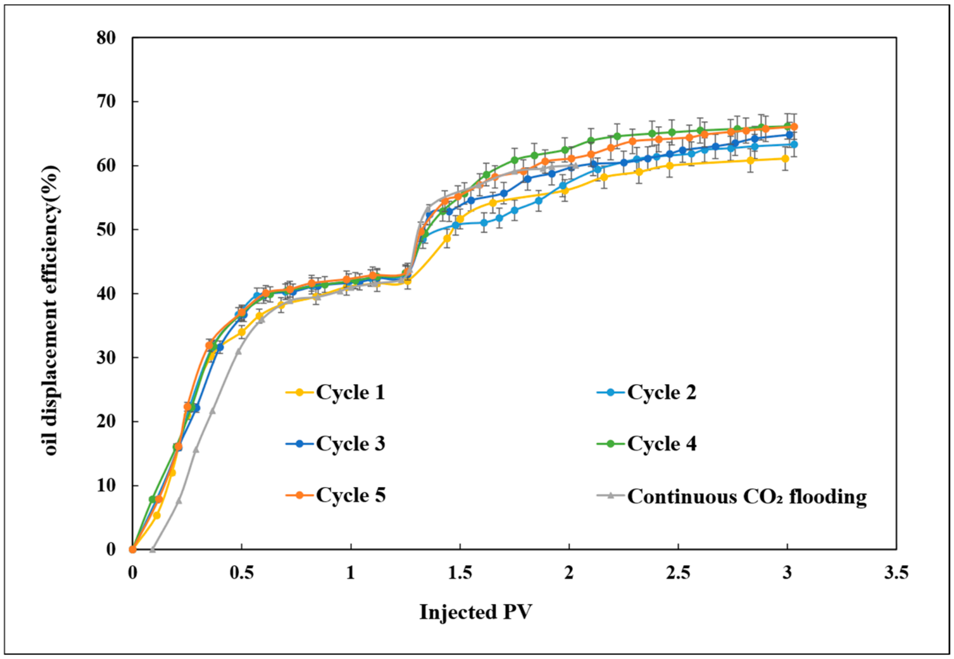

Figure 9: Oil displacement efficiency of KS core under continuous CO_2 flooding and different WAG cycles.

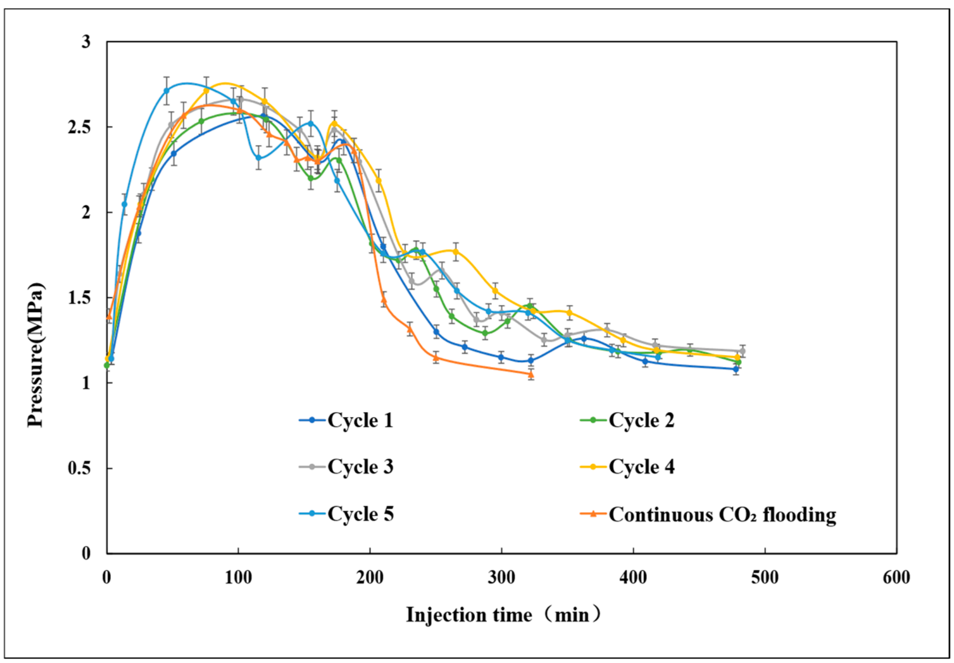

Figure 10: Differential pressure of KS core under continuous CO_2 flooding and different WAG cycles.

Experimental results shown in Fig. 11 indicate that the injection cycles have a significant regulatory effect on oil displacement efficiency. As the number of alternating cycles increased from 1 to 5, the final oil displacement efficiency of WAG gradually rose from 61.1% to 66.08%, and the increase compared to water flooding (oil displacement efficiency 41.3%) rose from 20.10% to 25.08%. The later the gas breakthrough time, the more the three phases of oil, gas and water come into full contact, which increases the oil-phase mobility ratio and reduces the viscosity of crude oil. When the injection cycles are 1 to 2, an increase in the single injection volume can easily cause CO_2 channeling, resulting in a decrease in oil displacement efficiency. When there are 4 to 5 injection cycles, the injection slug is smaller, the contact between CO_2 and crude oil is less, and the gas dissolution is smaller, which affects the development effect of the injection. Overall, three alternating cycles are the optimal parameters under the experimental conditions.

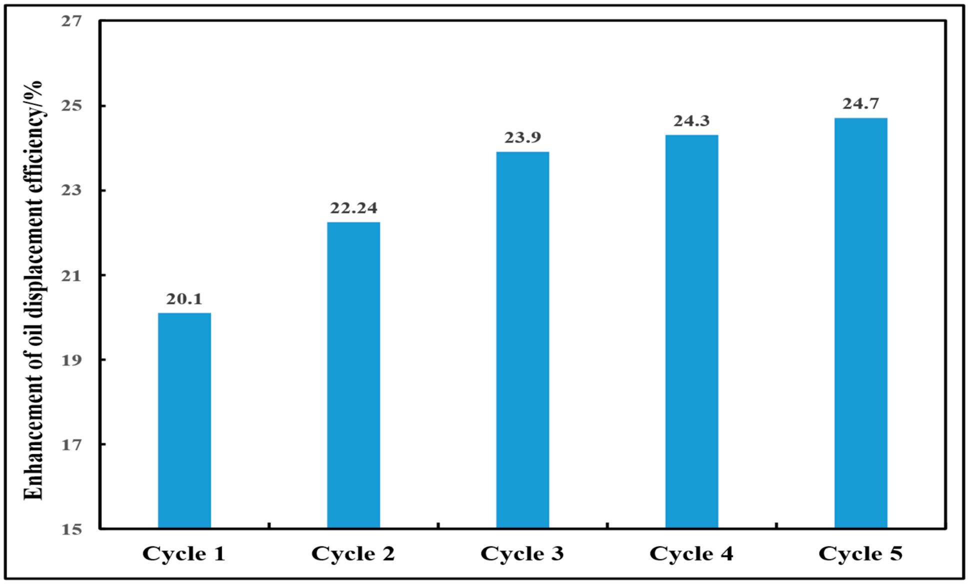

Figure 11: Enhancement of oil displacement efficiency by different CO_2-WAG cycle after water flooding.

(2) Experiments on CO_2-WAG displacement with different gas-water ratio

To study how the gas-water ratio affects CO_2 water-alternating-gas displacement, the injection volume ratio of CO_2 to water was changed. The ratios were set to 2:1, 1.5:1, 1:1, 1:1.5, and 1:2. Four cycles of gas-water alternating displacement were used for each ratio. Oil displacement efficiency, water cut, and gas-oil ratio were measured. Oil production, water production, and gas production were also recorded. Figs. 12–17 clearly show that the gas-water ratio has a large effect on the final oil displacement efficiency of the WAG process. As the gas-water ratio went down from 2:1 to 1:2, the final oil displacement efficiency of CO_2-water alternating flooding went up from 62.03% to 66.95%. The increase compared to water flooding grew from 21.13% to 25.45%. A lower gas-water ratio helps crude oil and CO_2 contact each other more fully. It also lowers the crude oil viscosity and delays the gas breakthrough time. A gas-water ratio of 1:2 raises oil displacement efficiency by 6.90% compared to continuous gas flooding. Notably, as the gas-water ratio goes up, the total injected pore volume increases. This increase leads to better displacement efficiency. When the gas-water ratio drops to 1:1 or below, the increase in oil displacement efficiency becomes smaller and slows down. This behavior comes from how the displacement phase controls fluidity and how the microscopic oil washing works under different gas-water ratios. A lower gas-water ratio means a higher proportion of water. This extra water helps control the flow of CO_2 and suppress gas channeling. As a result, the macroscopic sweep efficiency improves. However, a very high water ratio may also weaken the mass transfer and extraction between CO_2 and the crude oil underground. This weakening limits the gain in microscopic displacement efficiency.

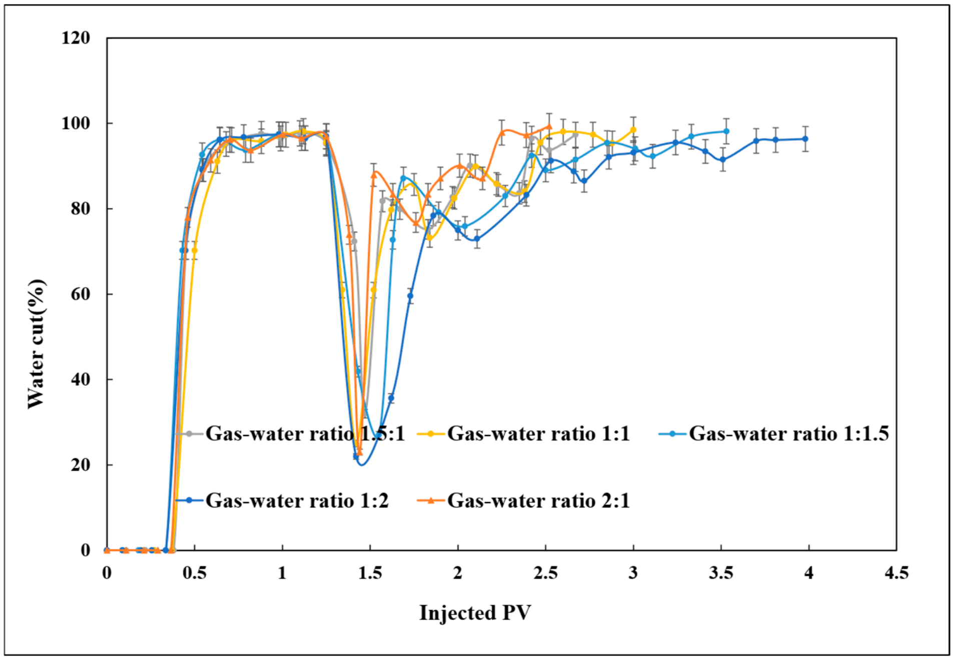

Figure 12: Water cut of KS core with different gas-water ratios.

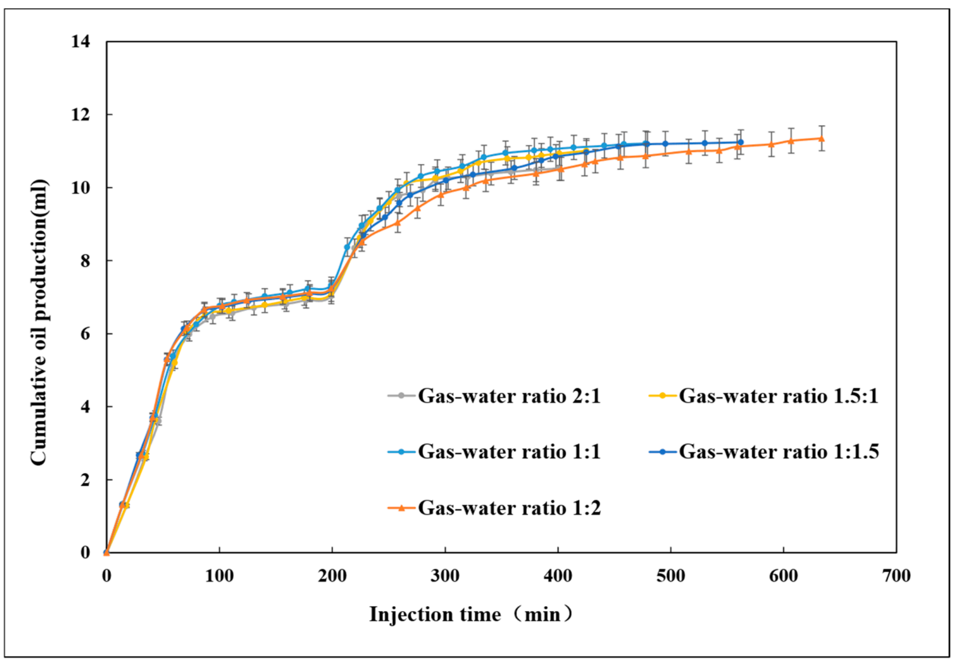

Figure 13: Cumulative oil production of KS core with different gas-water ratios.

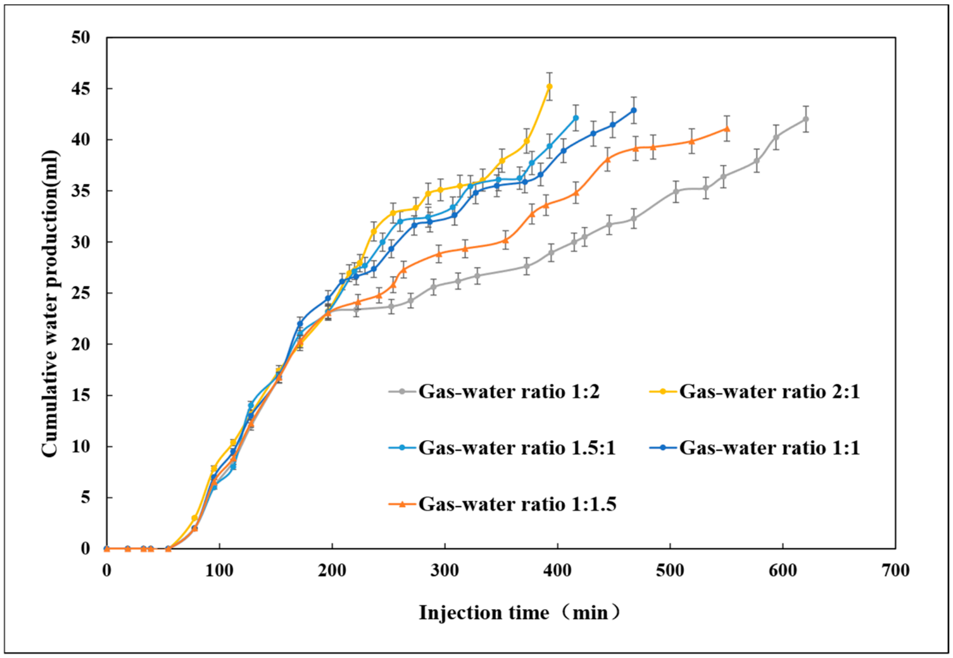

Figure 14: Cumulative water production of KS core with different gas-water ratios.

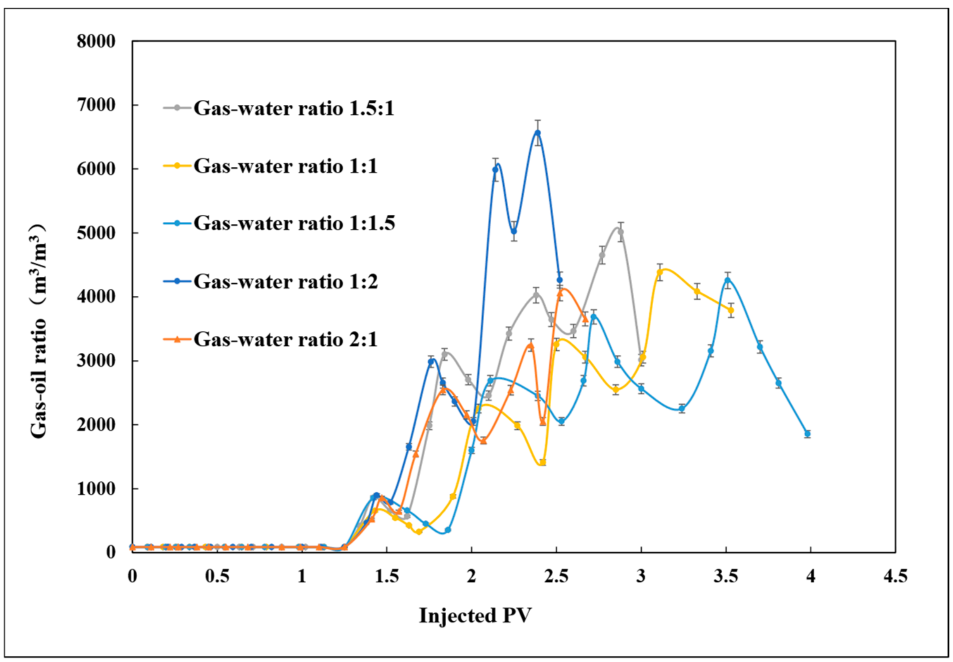

Figure 15: Gas-oil ratio of KS core with different gas-water ratios.

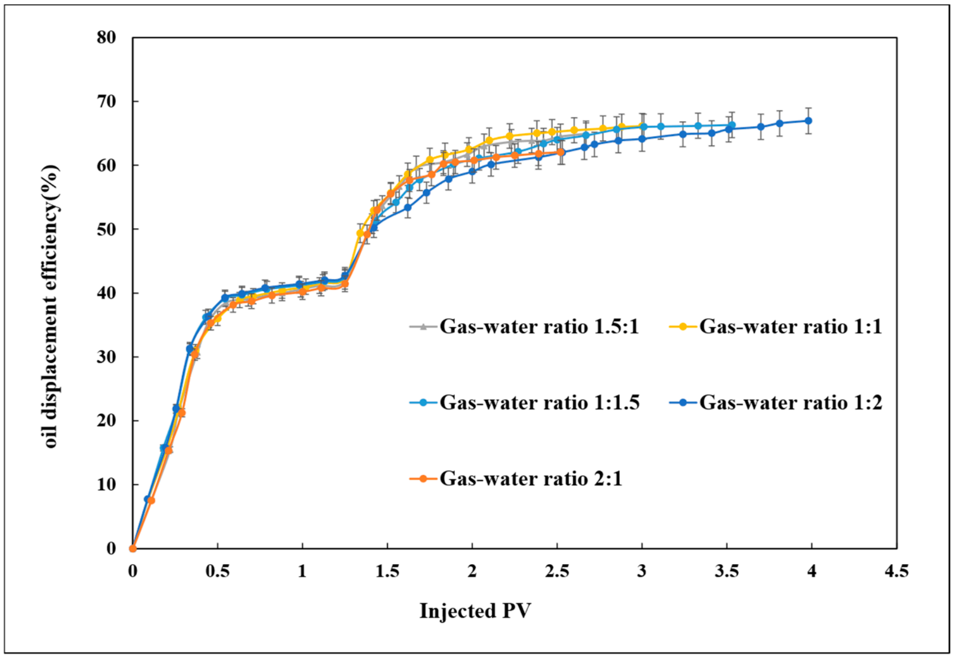

Figure 16: Oil displacement efficiency of KS core with different gas-water ratios.

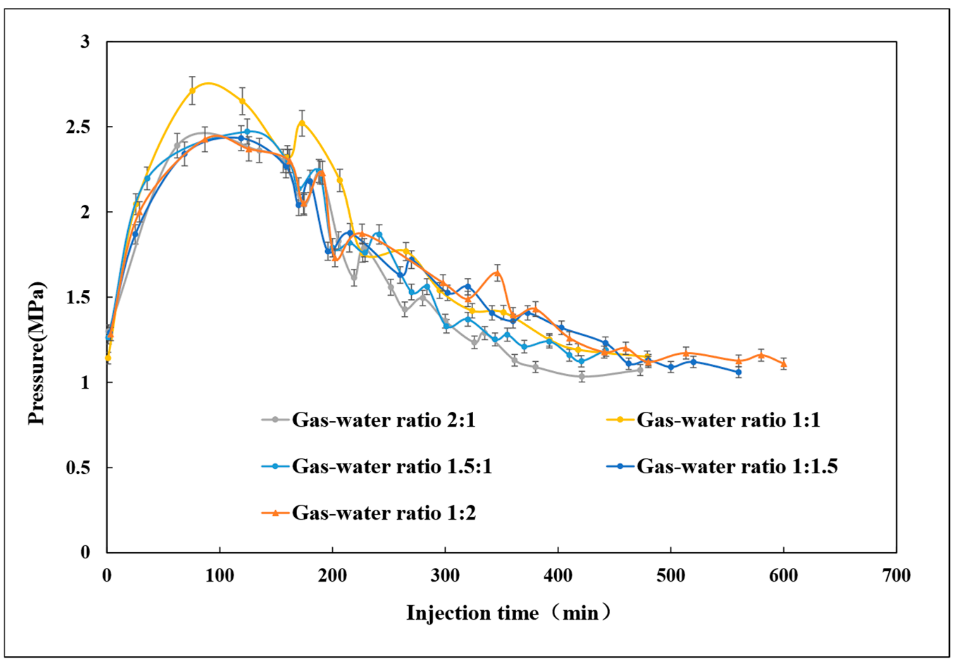

Figure 17: Differential pressure of KS core with different gas-water ratios.

As shown in Fig. 18, a gas-water ratio of 1:1 is an optimal injection parameter for the 9# core. It can form an effective CO_2 enrichment zone, fully reduce the viscosity and interfacial tension of crude oil, and control the flow rate of CO_2 through the water slug, allowing it sufficient time to diffuse into the micro-nano pore throat to interact with crude oil, thereby achieving a synergistic effect of macroscopic sweep and microscopic displacement.

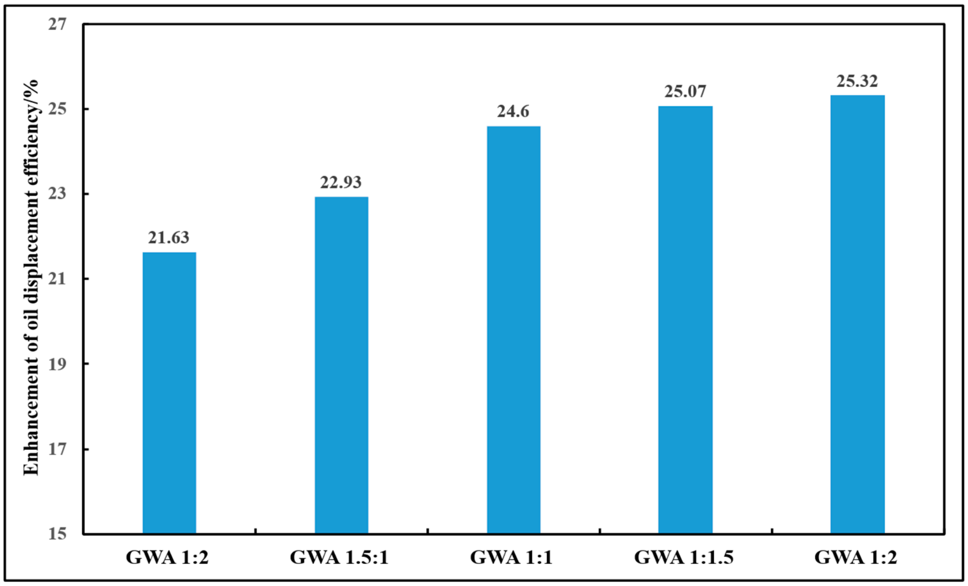

Figure 18: Enhancement of oil displacement efficiency by different gas-water ratio after water flooding.

(3) Error analysis and reliability

To ensure the reliability of the experimental results presented in Sections 1 and 2, we systematically evaluated potential sources of error across all eleven experimental scenarios: continuous CO_2 flooding, CO_2-WAG flooding at five different cycle numbers (1 to 5 cycles), and CO_2-WAG flooding at five different gas-water ratios (2:1, 1.5:1, 1:1, 1:1.5, and 1:2). The error analysis addresses experimental reproducibility, systematic and random errors, lithological modification during successive runs, and the quantified precision of the measurements.

① Systematic and Random Errors [24,25]: The pressure transducers employed for monitoring injection pressure, confining pressure, and differential pressure were calibrated prior to each experimental run. Liquid production was recorded using graduated cylinders, and readings were taken at regular intervals to minimize human reading errors. The injection pump was operated at a constant rate of 0.1 mL/min throughout all displacement experiments, and the back-pressure regulator maintained the outlet pressure at 20.1 MPa, consistent with the original reservoir formation pressure. At the pore scale, the Jamin effect—arising from gas bubble deformation as CO_2 traverses complex pore throats in the conglomerate formation—introduces inherent fluctuations in the differential pressure profiles. These transient pressure variations represent an intrinsic feature of multiphase flow in low-permeability porous media and do not affect the overall displacement trends.

② Lithological Modification: During successive experimental runs, we observed a gradual increase in average permeability of approximately 5%. We attribute this to the dissolution of carbonate cementing materials by carbonic acid generated *in situ* when dissolved CO_2 reacts with formation water under the experimental conditions of 20.1 MPa and 58°C. This permeability evolution is consistent with known geochemical interactions between CO_2-enriched brine and carbonate-cemented clastic rocks, and it accounts for the minor differences observed between successive runs on the same long core.

③ Quantified Precision: For the macroscopic production data—including oil displacement efficiency, water cut, gas-oil ratio, and cumulative oil, water, and gas production presented in Figs. 5–10 and 12–17—the error bars represent a relative error of 3%. The limited dispersion of the data across the eleven experimental groups confirms the reproducibility of the measurements and supports the validity of the optimized CO_2-WAG injection parameters identified in this study.

4 Online Nuclear Magnetic Resonance Displacement Experiment

In this section, the dynamic changes of fluid signals in the core under different CO_2 displacement methods were monitored in real time and *in situ* using online nuclear magnetic resonance technology, and the NMR transverse relaxation time (T_2) were converted into pore throat distributions, thereby quantitatively revealing the crude oil displacement patterns in pores of different scales, clarifying the microscopic distribution characteristics of the remaining oil and the lower limit of effectively swept pore throats for different displacement methods.

(1) Continuous CO_2 gas flooding

Aiming at the problem of unclear effective pore range for CO_2 flooding in Oilfield B, an online nuclear magnetic resonance experiment of converting water flooding to CO_2 flooding in the KS group core was carried out at 20.1 MPa and 58°C. The online nuclear magnetic resonance experiments clearly demonstrated the displacement of pores by continuous CO_2 flooding. As shown in Fig. 19, during the process of establishing the irreducible water saturation, the oil phase, as the non-wetting phase, preferentially enters the larger pores with less percolation resistance, and then enters the smaller pores. The T_2 spectrum of the core exhibits a bimodal distribution with a higher right peak, indicating that the crude oil is primarily distributed within two pore throat size ranges: 10–100 nm (small pore throats) and 0.1–10 μm (large pore throats). The subsequent water flooding process led to a decline in both peaks of the T_2 spectrum, but the decline in the right peak (the large pore throat) was much greater than that in the left peak (the small pore throat), indicating that the water flooding mainly utilized the crude oil in the large pore throat (>1 μm), with an effective pore lower limit of 18.2 nm. After continuous CO_2 injection, as the injection volume reached 2 PV, the T2 spectrum pattern changed to "the bimodal peaks became comparable in height", indicating that the crude oil signal in the small throat region was also significantly reduced. Quantitative analysis indicated that continuous CO_2 flooding significantly expanded the lower limit of effectively swept pore throats from 18.2 nm after water flooding to 11.6 nm, and the upper limit of exploitation was 34.6 μm.

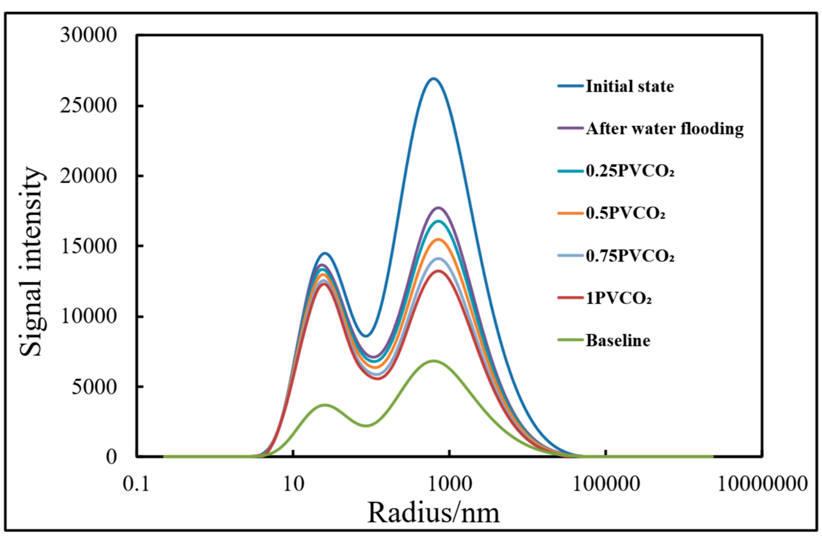

Figure 19: Online NMR experiment T_2 spectra of CO_2 flooding after water flooding of KS core.

Continuous CO_2 flooding can reach even smaller throats that water flooding cannot, and the core mechanism lies in the unique physicochemical effects of CO_2. When CO_2 gas is injected into the reservoir under high pressure, it dissolves rapidly in crude oil, causing the volume of crude oil to expand and significantly reducing the viscosity of crude oil, thereby greatly improving the fluidity of crude oil. At the same time, the mass transfer between CO_2 and crude oil can extract the light components in crude oil, further improving the fluidity of crude oil. The synergy of these effects enables CO_2, which has strong diffusion and permeation capabilities, to enter the micro-nanoscale pore throat network that the aqueous phase cannot effectively reach, overcoming greater capillary resistance and driving out the bound crude oil. However, continuous gas flooding is also prone to gas channeling due to unfavorable mobility ratio, and its macroscopic sweep efficiency is limited, with some pore throat areas still not effectively swept.

(2) Alternate water and gas flooding

Perform an online NMR experiment of alternating water and gas flooding on the same 9# core. As shown in Fig. 20, the left peak (representing the micropores) of the T_2 spectrum after CO_2-WAG displacement decreased to a lower level compared with the T_2 spectra after water flooding and continuous CO_2 flooding. The lower limit of effectively swept pore throats of CO_2-WAG flooding extends further to 9.52 nm. At the microscale, it also outperforms continuous CO_2 flooding in terms of its ability to mobilize reservoir pore structures, especially for the remaining oil in nanoscale pore throats. The injection of water slugs effectively controls CO_2 mobility, mitigating viscous fingering and premature gas channeling. This forces the injected CO_2 to divert into unswept regions of medium-to-low permeability. Furthermore, water slugs introduce the Jamin effect by plugging preferential flow paths, increasing flow resistance and enhancing macroscopic sweep efficiency.

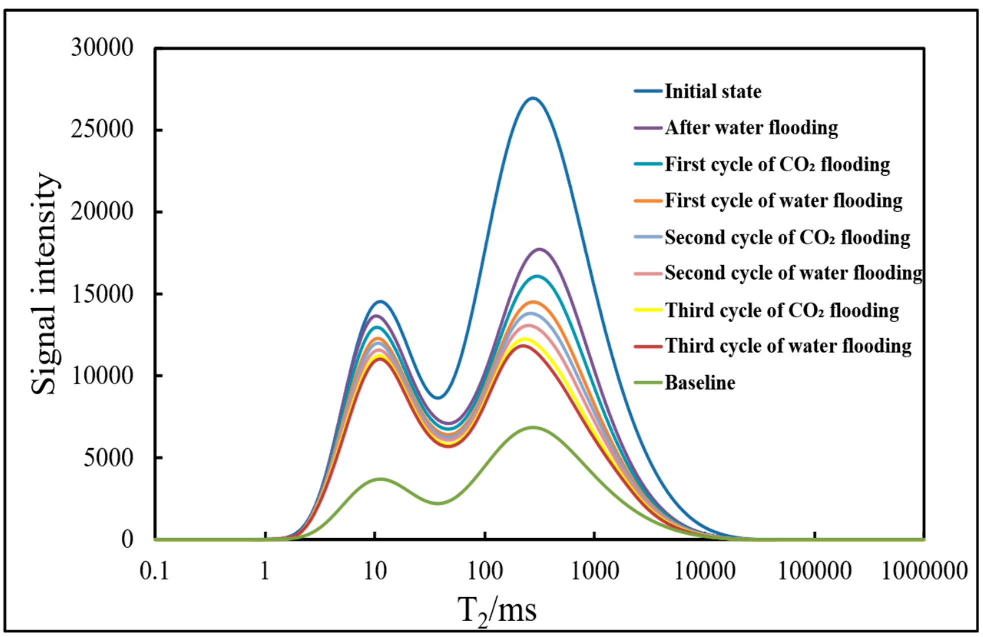

Figure 20: Online NMR experiment T_2 spectra of water and gas alternating flooding after water flooding of KS core.

The experimental results elucidate a distinct scale effect governing the multiphase flow mechanisms in low-permeability conglomerate reservoirs. At the microscopic scale, Nuclear Magnetic Resonance (NMR) analysis indicates that the Gas-WAG process significantly enhances the mobilization of residual oil within small pores (<100 nm). This phenomenon is primarily attributed to the microscopic Jamin effect, where the deformation of gas bubbles as they traverse pore throats generates fluctuating capillary pressures. These transient pressure variations are sufficient to overcome the adhesive forces binding the oil films to the pore walls.

However, at the macroscopic scale, this microscopic interaction manifests as a complex nonlinear increase in the pressure gradient. The alternating injection of immiscible phases (gas and water) induces severe phase interference, leading to a transient reduction in effective permeability. This behavior is quantitatively reflected in the relative permeability curves, characterized by a noticeable shift in the crossover point and a widening of the two-phase flow region. Consequently, the interplay between microscopic pore-scale mobilization and macroscopic fluid dynamic resistance dictates the overall displacement efficiency.

5 Conclusion

(1) In the low-permeability reservoir of the KS formation, the waterflooding development effect was limited. The final oil displacement efficiency was 41.3%, and the water cut rose above 95%, indicating that the water flooding sweep efficiency was limited and it was difficult to further improve the oil displacement efficiency. Online nuclear magnetic resonance shows that water flooding mainly recovers crude oil in macropores, with a lower limit of effectively swept pore throats of 18.2 nm. Crude oil in a large number of small pore throats (micro-nano pore throats <100 nm) is difficult to drive effectively and becomes the main space for remaining oil accumulation.

(2) Continuous CO_2 flooding can significantly improve flooding efficiency, but there is an obvious risk of gas channeling. Compared with water flooding, continuous CO_2 flooding increases oil displacement efficiency by 18.75%, but the gas-oil ratio rises rapidly during extraction, indicating significant gas channeling and the need for improvement in sweep efficiency. Compared with water flooding, continuous CO_2 flooding extends the lower limit of effectively swept pore throats from 18.2 nm to 11.6 nm, demonstrating that CO_2 can effectively drive the remaining oil in smaller micropores after reducing crude oil viscosity and interfacial tension. But the problem of its macroscopic sweep restricts the overall effect.

(3) The CO_2-water alternation drive is the best development approach in terms of overall effect, achieving the synergy of macroscopic sweep and microscopic displacement. The oil displacement efficiency increases with the number of alternating cycles, but slows down after more than three cycles. The oil displacement efficiency increases as the Gas-water ratio decreases, but the increase decreases below 1:1. The optimal injection parameters for CO_2-WAG injection are a 1:1 Gas-water ratio and three alternating cycles. Under this scheme, the final oil displacement efficiency can reach over 66%, which is 25% higher than that of water flooding and 5% higher than that of continuous gas flooding, and it can control the gas-oil ratio more effectively and suppress gas channeling. Online nuclear magnetic resonance experiments confirmed that under the WAG scheme, the lower limit of effectively swept pore throats of the KS conglomerate core was further extended to 9.52 nm, clearly revealing the superiority of gas-water alternating flooding over continuous gas flooding in micro-activation capacity. The water slug controls flow and expands macroscopic sweep, while the CO_2 slug reduces viscosity and extracts, and drives micropores. The two alternate and work together to break through the limitations of a single displacement method. Therefore, CO_2 gas-water alternating flooding can serve as an effective method for late-stage channeling prevention and enhanced oil recovery in high-water-cut and low-permeability reservoirs.

Acknowledgement: None.

Funding Statement: Technology Integration and Demonstration of CO_2 Miscible Flooding 609 in Water-Sensitive Low-Permeability Conglomerate Reservoirs (2025ZD1408403), Research on the Demonstration Project of the "Ballast Stone" in BaiKouQuan/WuXia Oilfields, a Science and Technology Project of the Oil and Gas and New Energy Branch of China National Petroleum Corporation (2023YQX10207) (Xiaoguang Wang), the Xinjiang "Tianshan Talent" Training Program (2022TSYCCX0050) (Xiaoguang Wang), Special Project of Xinjiang Oilfield Company on "Research and Field Test of Geological Reservoir Engineering for CO_2 Flooding in Junggar Basin" (2024XJZX0801) (Xiaoguang Wang), and the Natural Science Foundation of China (NSFC) (Grant No. 52504021) (Zongfa Li).

Author Contributions: The authors confirm contribution to the paper as follows: study conception and design: Xiaoguang Wang, Zhenping Liu; data collection: Zhen Luo, Guihua Yang; analysis and interpretation of results: Xiaoguang Wang, Dehua Liu; draft manuscript preparation: Xiaoguang Wang, Zongfa Li, Lijuan Huang. All authors reviewed and approved the final version of the manuscript.

Availability of Data and Materials: The data that support the findings of this study are available from the corresponding author upon reasonable request.

Ethics Approval: Not applicable.

Conflicts of Interest: The authors declare no conflicts of interest.

References

1. Ding M, Wang Y, Wang W, Zhao H, Liu D, Gao M. Potential to enhance CO_2 flooding in low permeability reservoirs by alcohol and surfactant as co-solvents. J Petrol Sci Eng. 2019;182:106305. [CrossRef].
2. Li Z, Gu Y. Soaking effect on miscible CO_2 flooding in a tight sandstone formation. Fuel. 2014;134:659–68. [CrossRef].
3. Zhao L, Sang G, Ding J, Sun J, Liu T, Yao Y. Research on the timing of WAG intervention in low permeability reservoir CO_2 flooding process to improve CO_2 performance and enhance recovery. Energies. 2023;16(21):7373. [CrossRef].
4. Qin Z, Arshadi M, Piri M. Micro-scale experimental investigations of multiphase flow in oil-wet carbonates. II. Tertiary gas injection and WAG. Fuel. 2019;257:116012. [CrossRef].
5. Afzali S, Ghamartale A, Rezaei N, Zendehboudi S. Mathematical modeling and simulation of water-alternating-gas (WAG) process by incorporating capillary pressure and hysteresis effects. Fuel. 2020;263:116362. [CrossRef].
6. Afzali S, Rezaei N, Zendehboudi S. A comprehensive review on enhanced oil recovery by water alternating gas (WAG) injection. Fuel. 2018;227:218–46. [CrossRef].
7. Khan MY, Mandal A. Analytical model for gravity segregation in WAG displacement recovery of inclined stratified reservoirs. J Petrol Sci Eng. 2020;186:106722. [CrossRef].
8. Valeev A, Shevelev A. Design of WAG parameters. In: Proceedings of the SPE Russian Petroleum Technology Conference; 2017 Oct 16–18; Moscow, Russia. [CrossRef].
9. Fang P, Zhang Q, Zhou C, Yang Z, Yu H, Du M, et al. Chemical-assisted CO_2 water-alternating-gas injection for enhanced sweep efficiency in CO_2-EOR. Molecules. 2024;29(16):3978. [CrossRef].
10. Abdurrahman M, Hidayat F, Husna UZ, Arsad A. Determination of optimum CO_2 water alternating gas (CO_2-WAG) ratio in Sumatera Light Oilfield. Mater Today Proc. 2021;39:970–4. [CrossRef].
11. Khather M, Myers M, Saeedi A, Giwelli A. Dissolution behaviour in carbonate reservoirs during WAG injection: a preliminary experimental study. E3S Web Conf. 2023;366:01007. [CrossRef].
12. Zhang D, Liu J, Liu S, Gong R, Li H. EOR mechanisms and influencing factors of CO_2-WAG immiscible displacement in heterogeneous sandy conglomerate reservoirs using nuclear magnetic resonance technology. Energy Proc. 2025;56:1–7. [CrossRef].
13. Al-Bayati D, Saeedi A, Ghasemi M, Arjomand E, Myers M, White C, et al. Evaluation of miscible CO_2 WAG/sandstone interactions: emphasis on the effect of permeability heterogeneity and clay mineral content. In:

Proceedings of the SPE Europec Featured at 81st EAGE Conference and Exhibition; 2019 Jun 3–6; London, UK. [CrossRef].

14. Li Y, Yang Y, Dong M, Wang J, Jing W, Yao J, et al. Micro-scale experimental investigations of CO_2-WAG injection and Ostwald ripening analysis in carbonate rocks with different pore structures. Geoenergy Sci Eng. 2024;241:213092. [CrossRef].
15. Sang G, Zhou Z, Gao W, Yin H, Chen H, Zhang F, et al. Mobilization characterization of remaining oil by CO_2 water-gas alternating after water flooding in low-permeability reservoirs. Phys Fluids. 2025;37(7):072006. [CrossRef].
16. Liu JR, Zhang DF, Liu SY, Gong RD, Wang L. Multiscale investigation into EOR mechanisms and influencing factors for CO_2-WAG injection in heterogeneous sandy conglomerate reservoirs using NMR technology. Petrol Sci. 2025;22(7):2977–91. [CrossRef].
17. Xu R, Wang S, Guo P, Hukuang H, Yuan N. Multi-scale investigation of CO_2-WAG injection mechanisms in water-sensitive tight oil reservoirs. Arab J Sci Eng. 2025;50(13):10327–44. [CrossRef].
18. Lang D, Lun Z, Lyu C, Wang H, Zhao Q, Sheng H. Nuclear magnetic resonance experimental study of CO_2 injection to enhance shale oil recovery. Petrol Explor Dev. 2021;48(3):702–12. [CrossRef].
19. Li S, Zhang Y, Wang N, Wang Z, Liu H. Pore-scale investigation of water-alternating-gas injection for CCUS in water-wet porous media. Energy Fuels. 2025;39(6):3039–55. [CrossRef].
20. Zheng X, Lin Y, Cao R, Xiong Y, Cheng L, Jia Z. Potential evaluation of enhanced oil recovery and CO_2 storage in fractured tight reservoirs using CO_2-WAG technology based on core-scale experiments and numerical simulation. In: Proceedings of the SPE Asia Pacific CCUS Conference; 2025 Aug 26–27; Kuala Lumpur, Malaysia. [CrossRef].
21. Wang Y, Chang T, Zhou J, Wu J, Liu S. Remaining oil distribution characteristics in sandy conglomerate reservoirs during CO_2-WAG flooding: insights from nuclear magnetic resonance (NMR) technology. Processes. 2025;13(9):2872. [CrossRef].
22. He J, Ke W, Zhu X, Zhen M, Liu T. Research on enhanced oil recovery by CO_2–water/polymer composite alternative flooding in heterogeneous reservoirs. ACS Omega. 2025;10(43):51272–83. [CrossRef].
23. Wang Q, Yang S, Lorinczi P, Glover PWJ, Lei H. Experimental investigation of oil recovery performance and permeability damage in multilayer reservoirs after CO_2 and water–alternating-CO_2 (CO_2-WAG) flooding at miscible pressures. Energy Fuels. 2020;34(1):624–36. [CrossRef].
24. Chen H, Ma T, Shen L, Ye B, Ni S, Ni X, et al. Negative sample selection for landslide susceptibility prediction: a hybrid optimization approach using an AHP-KDE multi-ring sampling strategy. Ecol Indic. 2025;180:114304. [CrossRef].
25. Chen H, Ma T, Shen L, Liu Z, Ni S, Sun H. Assessmentof debris flow susceptibility based on PCA-IV coupling method and SHAP model: a case study of Linan District. Trans GIS. 2025;29(7):e70146. [CrossRef].